55 A COMPARISON OF DIFFERENT CRACK MODELS APPLIED TO PLAIN AND REINFORCED CONCRETE

P.H. FEENSTRA
Department of Civil Engineering, Delft University of Technology, The Netherlands
R. de BORST and J.G. ROTS
Department of Civil Engineering, Delft University of Technology, and TNO Building and Construction Research, Rijswijk, The Netherlands

Abstract
The paper describes two crack models embedded in a total strain concept, the fixed orthogonal crack model and the coaxial rotating crack model. These two crack models are compared with the corresponding crack models embedded in a decomposed strain concept. Further, a model for reinforced concrete based on a total strain concept is presented. The salient feature in this model is the stress decomposition into a stress contribution of the concrete with a strain softening model, a stress contribution of the reinforcing steel with a elasto-plastic model and a stress contribution owing to the interaction between concrete and reinforcement. The model capabilities are demonstrated in a simulation of a unidirectionally reinforced concrete panel.
Keywords : Rotating Crack Model, Fixed Crack Model, Reinforced Concrete Panels, Tension-stiffening, Tension-softening, Bond.

1. Introduction

Fracture of concrete can be modeled following several approaches. One of the most promising approaches for implementation in a finite element program is the phenomenological approach, in which fracture is described within a continuum. This approach is known as the smeared crack model. Generally an elastic-softening behavior is assumed in which a gradual decrease of the stress occurs after the crack is initiated. These constitutive models can be embedded in different concepts. In this study two concepts will be used, the decomposed strain concept and the total strain concept. The first concept is based on a strain decomposition into an elastic part and an inelastic part: $\boldsymbol{\varepsilon} = \boldsymbol{\varepsilon}^{el} + \boldsymbol{\varepsilon}^{cr}$. This model has been treated comprehensively in the work of de Borst and Nauta (1985) and Rots (1988), and will not be treated in this paper. The second concept is the total formulation in which the stress is assumed to be a function of the total strain. The constitutive behavior of models embedded in both concepts is highly dependent upon the modeling of the shear stress-strain relation. This has resulted in different crack models, the fixed smeared crack model and the rotating smeared crack model. In this study the fixed and the rotating crack model embedded in a total strain concept will be treated.

The practical application of fracture models for concrete generally concerns reinforced concrete panels. The major characteristics of reinforced concrete are the distributed fracture in the neighborhood of the reinforcing bars and the localized fracture some distance away from the reinforcement. Especially in unidirectionally reinforced concrete panels this phenomenon becomes very challenging when cracks occur which are inclined at some angle with the reinforcement. This study deals with the gradual transition between the localized fracture in the unreinforced direction and the distributed fracture in the reinforced direction.

Fracture Processes in Concrete, Rock and Ceramics Edited by J.G.M. van Mier, J.G. Rots and A. Bakker.
 ISBN 0 419 15870 7

2. Crack models in a total strain concept

In smeared crack models a crack is conceived to be distributed over the area of an element represented by an integration point. With this approach the cracked material is considered as a continuum, for which the notions of stress and strain are defined. This means that the constitutive relation can be described in terms of stress-strain relations. Commonly, and this has also been done in this study, the constitutive relation in the uncracked state is restricted to linear-elasticity. When a tension cut-off criterion is violated, this linear-elastic relation is replaced by an orthotropic stress-strain law with the axes of orthotropy in accordance with the directions of the principal stresses. The explicit application of the orthotropic elasticity theory to cracked concrete is not straightforward. Indeed, the concept of a fully orthotropic material has not yet been applied to describe smeared cracking. Instead, it is assumed that cracking only influences the diagonal terms in the compliance matrix (Bažant and Oh, 1983). Then the total stress-strain relation in a plane-stress configuration is given by the following stiffness relation in the crack coordinate system n,s :

$$\sigma_{n,s} = \mathbf{D}_{n,s}\, \varepsilon_{n,s} \tag{1}$$

with

$$\mathbf{D}_{n,s} = \begin{bmatrix} \dfrac{\alpha_n E}{1-\alpha_n\alpha_s\nu^2} & \dfrac{\alpha_s\alpha_n E}{1-\alpha_n\alpha_s\nu^2} & 0 \\ \dfrac{\alpha_n\alpha_s E}{1-\alpha_n\alpha_s\nu^2} & \dfrac{\alpha_s E}{1-\alpha_n\alpha_s\nu^2} & 0 \\ 0 & 0 & \beta_s G \end{bmatrix} \tag{2}$$

As a first approximation it is assumed that the reduction factors α_n, α_s for the elastic Young's modulus E are only functions of the tensile strains in the considered directions, i.e. $\alpha_n = \alpha_n(\varepsilon_{nn})$, $\alpha_s = \alpha_s(\varepsilon_{ss})$ and $\beta_s = \beta_s(\gamma_{ns})$.

The constitutive relation, eq.(1), has been expressed in the local coordinate system. Using the strain transformation matrix $\mathbf{T}(\phi)$ the relation in the global coordinate system is given by:

$$\sigma_{x,y} = [\,\mathbf{T}(\phi)^T\, \mathbf{D}_{n,s}\, \mathbf{T}(\phi)]\, \varepsilon_{x,y} \tag{3}$$

in which the superscript T denotes the transpose and ϕ is the angle between the local crack coordinate system and the global coordinate system. The tangential stiffness matrix is always needed in a non-linear analysis which employs a Newton-Raphson type iterative procedure. These stiffness moduli may be readily obtained by differentiating:

$$\sigma_{x,y} = \mathbf{T}^T(\phi)\, \sigma_{n,s} \tag{4}$$

which results in:

$$\dot{\sigma}_{x,y} = {}^t\mathbf{D}_{x,y}\, \dot{\varepsilon}_{x,y} \tag{5}$$

with ${}^t\mathbf{D}_{x,y}$ the tangent stiffness matrix

$${}^t\mathbf{D}_{x,y} = \left[\, \mathbf{T}^T(\phi)\, \frac{\partial\sigma_{n,s}}{\partial\varepsilon_{n,s}}\, \mathbf{T}(\phi) + \frac{\partial\mathbf{T}^T(\phi)}{\partial\phi}\, \sigma_{n,s}\, \frac{\partial\phi^T}{\partial\varepsilon_{x,y}} \,\right] \tag{6}$$

2.1 Fixed crack model

In the fixed crack model the principal axes of orthotropy are kept fixed during the post-cracking phase. This results in the following constitutive model:

$$\sigma_{x,y} = [\, \mathbf{T}^T(\phi_0)\, \mathbf{D}_{n,s}\, \mathbf{T}(\phi_0)]\, \varepsilon_{x,y} \tag{7}$$

in which ϕ_0 the angle between the global coordinate system and the crack coordinate system. Because $\partial \mathbf{T}^T / \partial \phi = \mathbf{0}$, the tangential stiffness matrix reads explicitly

$${}^t\mathbf{D}_{x,y} = \mathbf{T}^T(\phi_0) \begin{bmatrix} \partial\sigma_{nn}/\partial\varepsilon_{nn} & \partial\sigma_{nn}/\partial\varepsilon_{ss} & 0 \\ \partial\sigma_{ss}/\partial\varepsilon_{nn} & \partial\sigma_{ss}/\partial\varepsilon_{ss} & 0 \\ 0 & 0 & \partial\sigma_{ns}/\partial\gamma_{ns} \end{bmatrix} \mathbf{T}(\phi_0) \tag{8}$$

This model has also been used by Rots, Nauta, Kusters and Blaauwendraad (1985) as an extension of the fixed crack model proposed by Bažant and Oh (1983). A more fundamental treatment of the fixed crack model is given in the inspirational work of Willam, Pramono and Sture (1987).

2.2 Rotating crack model

The rotating crack model differs notably from the fixed crack model in the post-cracking phase. The principal axes of orthotropy are not kept constant, but rotate coaxially with the principal strains during crack propagation. The constitutive model is now defined by the full expression of eq.(3) with $\mathbf{T}(\phi)$ a function of the global strains. The tangential stiffness matrix ${}^t\mathbf{D}_{x,y}$, is more complicated because of the introduction of the spin of the principal stress axes and is given by the full expression of eq.(6). The first term of the tangential stiffness matrix is equal to the tangential stiffness matrix that follows from the fixed crack approach, and can be considered as the material tangent stiffness. The second term, due to the spin of the principal axes, is a function of the stresses and the angle ϕ between global coordinate system and crack coordinate system. The rotating crack model does not involve an independent shear-retention factor β, but the coaxiality condition results in a shear stiffness that is associated with the rotation of the principal axes. Many authors, e.g. Bažant (1983), Crisfield and Wills (1989) and Willam, Pramono and Sture (1987), have proved that in a two-dimensional configuration ${}^t\mathbf{D}_{x,y}$ can then be written as:

$${}^t\mathbf{D}_{x,y} = \mathbf{T}^T(\phi) \begin{bmatrix} \partial\sigma_{nn}/\partial\varepsilon_{nn} & \partial\sigma_{nn}/\partial\varepsilon_{ss} & 0 \\ \partial\sigma_{ss}/\partial\varepsilon_{nn} & \partial\sigma_{ss}/\partial\varepsilon_{ss} & 0 \\ 0 & 0 & (\sigma_{nn}-\sigma_{ss})/2(\varepsilon_{nn}-\varepsilon_{ss}) \end{bmatrix} \mathbf{T}(\phi) \tag{9}$$

3. Tension - shear model problem

To verify the elastic-softening formulations for the fixed and the rotating crack models, reference is made to the plane-stress model problem of biaxial tension and shear depicted in Figure 1 (Willam, Pramono and Sture, 1987 ; Rots 1988). It concerns an elastic-softening continuum of unit dimensions with a Young's modulus $E = 10000\ [N/mm^2]$, Poisson's ratio $\nu = 0.2$, tensile strength $f_{ct} = 1.0\ [N/mm^2]$ and a fracture energy $G_f = 0.15\ [Nmm/mm]$ over a unit crack band width $h = 1.0\ [mm]$. Initially, the continuum is subjected to tensile straining in the x-direction accompanied by lateral Poisson contraction in the y-direction, i.e. $\Delta\varepsilon_{xx} : \Delta\varepsilon_{yy} : \Delta\gamma_{xy} = 1 : -\nu : 0$. Immediately after cracking, a switch is made to combined biaxial tension and shear according to $\Delta\varepsilon_{xx} : \Delta\varepsilon_{yy} : \Delta\gamma_{xy} = 0.5 : 0.75 : 1$, which causes the axes of principal strain to continuously rotate after cracking as is typical of fracture propagation in smeared finite element models. For both concepts an analysis has been made for both the fixed crack model as well as the coaxial rotating crack model. In the figures the following abbreviations have been used to indicate the different crack models in the two strain concepts:

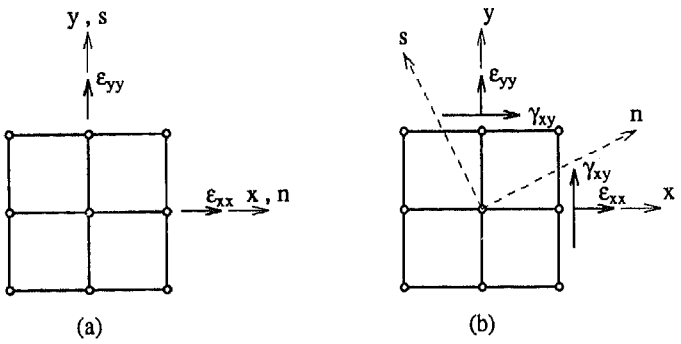

Figure 1 Lay-out tension-shear model problem.
(a) tension up to cracking;
(b) biaxial tension with shear beyond cracking

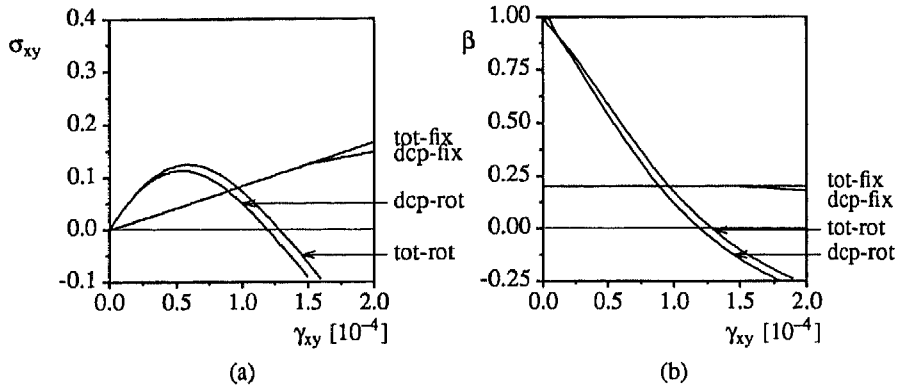

Figure 2 Behavior in shear for different strain concepts and crack models.
(a) shear stress-strain response in x,y-direction;
(b) shear retention factor $\beta = \sigma_{xy} / (G \gamma_{xy})$

decomposed strain concept with a fixed crack model: dcp-fix; decomposed rotating crack model: dcp-rot; total strain concept with a fixed crack model: tot-fix and total rotating crack model: tot-rot. The nominal $\sigma_{xy} - \gamma_{xy}$ shear response is shown in Figure 2(a). The fixed crack models both give a linear relation because of the constant shear-retention factor β. The equivalent shear-retention factor is given in Figure 2(b). This secant shear-retention factor is extracted from the stresses and strains in the global coordinate system. For the rotating crack models the results show that the shear-retention factor rapidly decreases and even becomes negative. The decomposed strain concept shows a small deviation compared with the total strain concept when a second crack arises. For the total formulation the shear stiffness is independent from the cracks in both directions. For the decomposed formulation the shear stiffness for each crack is dependent upon the shear-retention factor and this results in a decrease of the shear stiffness at the element level. The normal stress-strain response in the global coordinate system is depicted in Figure 3. The decomposed strain concept with a fixed crack model results in a

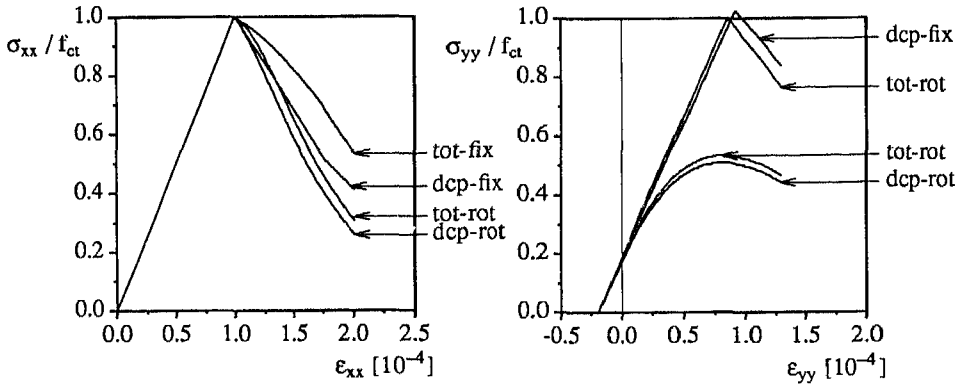

Figure 3 Normal stress-strain response in x-direction and y-direction, for different strain concepts and crack models.

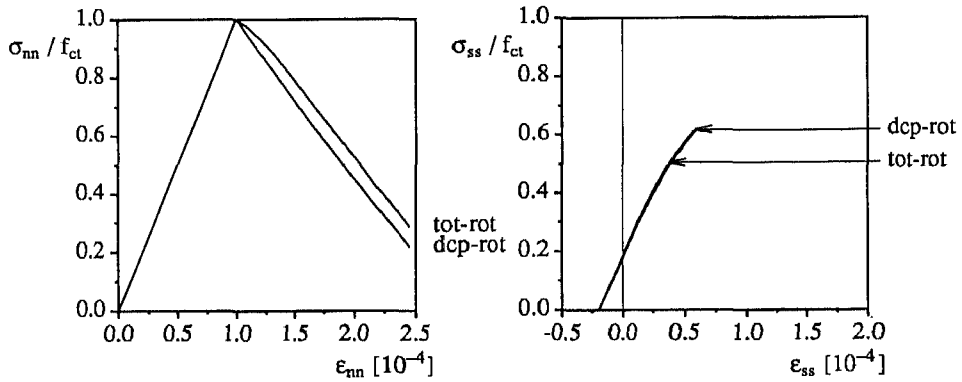

Figure 4 Principal tensile stress-strain response in n,s-direction for different strain concepts and a rotating crack model.

$\sigma_{xx} - \varepsilon_{xx}$ diagram which, until the second crack arises, is equivalent to the input softening diagram. The large deviation between the total and the decomposed strain concept for the fixed crack model is surprising, especially since, for the rotating crack model, both strain concepts give results that are in reasonable agreement. The $\sigma_{yy} - \varepsilon_{yy}$ response shows the the degradation of the strength in the lateral direction. The principal stress-strain response is depicted in Figure 4 for the rotating crack model. The principal stress-strain response for the fixed crack model has no physical meaning, since the directions of the principal strain and the principal stress are not equal. The $\sigma_{nn} - \varepsilon_{nn}$ response shows the linear softening diagram since the softening is explicitly monitored in the rotating, principal strain coordinate system. The deviation between the total and the decomposed strain concept is a result of the Poisson effect. The stress-strain diagram in the lateral direction $\sigma_{ss} - \varepsilon_{ss}$ shows that the lateral stresses remain small during the total loading process.

4. Constitutive model for reinforced concrete

The constitutive model for reinforced concrete assumed in this study is based on the assumption that reinforced concrete is a composite material. With this assumption it is possible to decompose the total stress in the stress components of the constituent materials, concrete and steel, and a stress component due to the interaction between concrete and steel. The reinforcing steel is modeled with an embedded formulation in which it is assumed that the strain for both materials is equal. The total stress is now given by:

$$\boldsymbol{\sigma}_{x,y} = \boldsymbol{\sigma}^{c}_{x,y} + \boldsymbol{\sigma}^{s}_{x,y} + \boldsymbol{\sigma}^{ia}_{x,y} \tag{10}$$

in which the superscript c denotes the concrete, s the reinforcing steel and ia the stresses due to the interaction between concrete and reinforcement. The constitutive relation for the concrete has already been derived (cf. eq.(3)):

$$\boldsymbol{\sigma}^{c}_{x,y} = [\mathbf{T}^{T}(\phi)\, \mathbf{D}_{n,s}\, \mathbf{T}(\phi)\,]\, \boldsymbol{\varepsilon}_{x,y}$$

The constitutive relation for the reinforcing steel looks very similar:

$$\boldsymbol{\sigma}^{s}_{x,y} = [\,\mathbf{T}^{T}(\theta)\, \mathbf{D}_{s}\, \mathbf{T}(\theta)\,]\, \boldsymbol{\varepsilon}_{x,y} \tag{11}$$

with θ the inclination angle between the reinforcing grid and the global x,y-coordinate system. The constitutive relation for the reinforcing grid is given by the matrix:

$$\mathbf{D}_{s} = \begin{bmatrix} \rho_{p} E_{s}^{ep} & 0 & 0 \\ 0 & \rho_{q} E_{s}^{ep} & 0 \\ 0 & 0 & 0 \end{bmatrix} \tag{12}$$

with the reinforcing ratios ρ_p, ρ_q in the p, q directions of the grid respectively and E_s^{ep} the secant elasto-plastic modulus.

The stress contribution owing to the interaction between concrete and reinforcement is given by:

$$\boldsymbol{\sigma}^{ia}_{x,y} = \mathbf{T}^{T}(\phi)\, \boldsymbol{\sigma}^{ia}_{n,s} \tag{13}$$

The stresses on the crack surface are in general functions of the angle between the reinforcement and the normal on the crack surface. For the first crack in the n-direction this transformation yields:

$$\begin{Bmatrix} \sigma_{nn} \\ \sigma_{ss} \\ \sigma_{ns} \end{Bmatrix}^{ia}_{1} = \begin{bmatrix} \cos\alpha & 0 & 0 \\ 0 & 0 & 0 \\ 0 & 0 & \cos\alpha \end{bmatrix} \begin{Bmatrix} \sigma_{pp} \\ \sigma_{qq} \\ \sigma_{pq} \end{Bmatrix}^{ia}_{1} + \begin{bmatrix} 0 & -\sin\alpha & 0 \\ 0 & 0 & 0 \\ 0 & 0 & \sin\alpha \end{bmatrix} \begin{Bmatrix} \sigma_{pp} \\ \sigma_{qq} \\ \sigma_{qp} \end{Bmatrix}^{ia}_{1} \tag{14}$$

with the angle α the angle between reinforcement and the normal of the crack. For the possible second crack in the s-direction the transformation of the stresses in the reinforcement direction to the crack coordinate system yields:

$$\begin{Bmatrix} \sigma_{nn} \\ \sigma_{ss} \\ \sigma_{ns} \end{Bmatrix}^{ia}_{2} = \begin{bmatrix} 0 & 0 & 0 \\ \sin\alpha & 0 & 0 \\ 0 & 0 & -\sin\alpha \end{bmatrix} \begin{Bmatrix} \sigma_{pp} \\ \sigma_{qq} \\ \sigma_{pq} \end{Bmatrix}^{ia}_{2} + \begin{bmatrix} 0 & 0 & 0 \\ 0 & \cos\alpha & 0 \\ 0 & 0 & \cos\alpha \end{bmatrix} \begin{Bmatrix} \sigma_{pp} \\ \sigma_{qq} \\ \sigma_{pq} \end{Bmatrix}^{ia}_{2} \tag{15}$$

The constitutive relation for the interaction stress in the p-direction of the reinforcement grid is given by:

$$\begin{Bmatrix} \sigma_{pp} \\ \sigma_{qq} \\ \sigma_{pq} \end{Bmatrix}_i = \begin{bmatrix} E_{bp,i} & 0 & 0 \\ 0 & 0 & 0 \\ 0 & 0 & E_{dp,i} \end{bmatrix} \begin{Bmatrix} \varepsilon_{pp} \\ \varepsilon_{qq} \\ \gamma_{pq} \end{Bmatrix} \tag{16}$$

and the stress in the q-direction of the grid:

$$\begin{Bmatrix} \sigma_{pp} \\ \sigma_{qq} \\ \sigma_{qp} \end{Bmatrix}_i = \begin{bmatrix} 0 & 0 & 0 \\ 0 & E_{bq,i} & 0 \\ 0 & 0 & E_{dq,i} \end{bmatrix} \begin{Bmatrix} \varepsilon_{pp} \\ \varepsilon_{qq} \\ \gamma_{pq} \end{Bmatrix} \tag{17}$$

The stiffness moduli E_{bp} and E_{bq} are the result of the bond stresses between the reinforcement and the concrete between the cracks. This contribution to the stiffness of the structure is commonly known as the tension-stiffening effect. The tension-stiffening moduli E_{bp} and E_{bq} are functions of the strain in the reinforcement and the strain in the crack coordinate system. This tension stiffening component is assumed to be a trilinear function, according to Cervenka, Pukl and Eligehausen (1990), see Figure 5(a). At ε_0 the crack arises and the ascending branch coincides with the softening of the concrete until the ultimate crack strain ε_u. The constant part is a fraction of the tensile strength of concrete, as a rough approximation 0.4 f_{ct}. The descending branch starts when the yielding of the reinforcement begins at a yield stress f_{sy} and a yield strain ε_{sy}.

The stiffness moduli E_{dp} and E_{dq} are the dowel stiffnesses of the reinforcement bars. These stiffness moduli are dependent upon the bar diameter, the crack width, the stress of the reinforcement and possibly on other parameters as well. In this study the dowel stiffness is assumed to be a fraction of the shear stiffness G_s of the reinforcement bar, $E_{dp} = E_{dq} = \delta \rho G_s$, $0 \le \delta \le 1$.

The tangential formulation of the stress components in reinforced concrete is essential for the solution of the nonlinear equations via a Newton-Raphson method. The tangential formulation is obtained by differentiation of the total stress-strain relation. For the concrete the tangential formulation has already been derived, eq.(5) and eq.(6). The tangential formulation for the reinforcement reads

$$\dot{\boldsymbol{\sigma}}^s_{x,y} = [\, \mathbf{T}^T(\theta)\, {}^t\mathbf{D}_s \mathbf{T}(\theta)\,]\, \dot{\boldsymbol{\varepsilon}}_{x,y} \tag{18}$$

in which the tangent operator for the grid is given by the matrix

$${}^t\mathbf{D}_s = \begin{bmatrix} \rho_p\, {}^tE_s^{ep} & 0 & 0 \\ 0 & \rho_q\, {}^tE_s^{ep} & 0 \\ 0 & 0 & 0 \end{bmatrix} \tag{19}$$

where ${}^tE_s^{ep}$ is the tangential elasto-plastic modulus: ${}^tE_s^{ep} = d\sigma_i / d\varepsilon_i$.

The tangent operator of the interaction stresses is more complicated because of the rotation of the crack direction if a rotating crack model is used. Using the formulation of the interaction stresses of eq.(13), the total derivative is given by

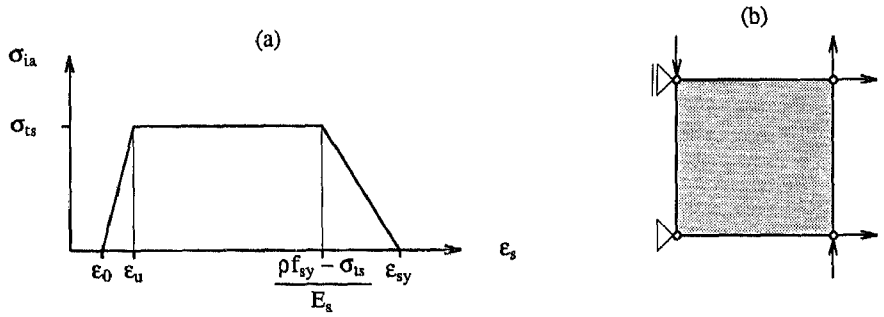

Figure 5 (a) Modeling of the tension-stiffening effect;
(b) Model panel Bhide and Collins (1987).

$$\dot{\sigma}^{ia}_{x,y} = \left[T^T(\phi) \frac{\partial \sigma^{ia}_{n,s}}{\partial \varepsilon_{x,y}} + \frac{\partial T^T(\phi)}{\partial \phi} \sigma^{ia}_{n,s} \frac{\partial \phi^T}{\partial \varepsilon_{x,y}} \right] \dot{\varepsilon}_{x,y} \tag{20}$$

in which the stress in the crack direction $\sigma^{ia}_{n,s}$ is given by eq.(14) for the first crack and eq.(15) for the second crack. The partial derivatives of these stress components with regard to the global strain vector result in a complicated formulation of the tangent stiffness operator for the interaction stress component of the total stress vector, Feenstra (1991).

5. Panel PB21 Bhide and Collins

Numerical experiments with the above described model for reinforced concrete were carried out for panel PB21 of Bhide and Collins (1987), with dimensions 870x870x70 [mm^3], a reinforcement percentage of 2.195 % in the element x-direction and a reinforcement percentage of 0.0 % in the element y-direction. The concrete has been modeled with a Young's modulus E_c = 20000 [N/mm^2], Poisson's ratio ν = 0.2, tensile strength f_{ct} = 2.0 [N/mm^2] and a fracture energy G_f = 0.89 [Nmm/mm] over a crack band width of 890 [mm]. A crack spacing of 100 [mm] has been assumed which means that approximately 9 cracks are distributed over the element size. The total amount of energy consumed in the panel is then 8.9 times the fracture energy for one crack. The total strain concept and linear tension softening have been used. Both the rotating crack model and the fixed crack model have been utilized. For the latter model a shear retention factor β = 0.2 has been adopted. The reinforcing steel has been modeled with a linear-elastic plastic model with a Young's modulus E_s = 210000 [N/mm^2] and a yield stress f_{sy} = 402 [N/mm^2]. The deformed bars of the reinforcing grid can sustain much more bond stress than plain bars. These bond characteristics have been modeled with a maximum bond stress of 1.4 [N/mm^2]. The dowel action and the nonlinearity in compression have been neglected. The finite element configuration for the analysis is one four-noded element with four integration points for both the reinforcement and the concrete, see Figure 5(b). The analyses have been performed under arc-length control. The results of the analyses are given in Figure 6 which shows the nominal shear stress-principal tensile strain diagram.

6. Concluding remarks

The crack models embedded in a total strain concept and a decomposed strain concept show reasonable agreement when the models are applied to a tension-shear model problem. The

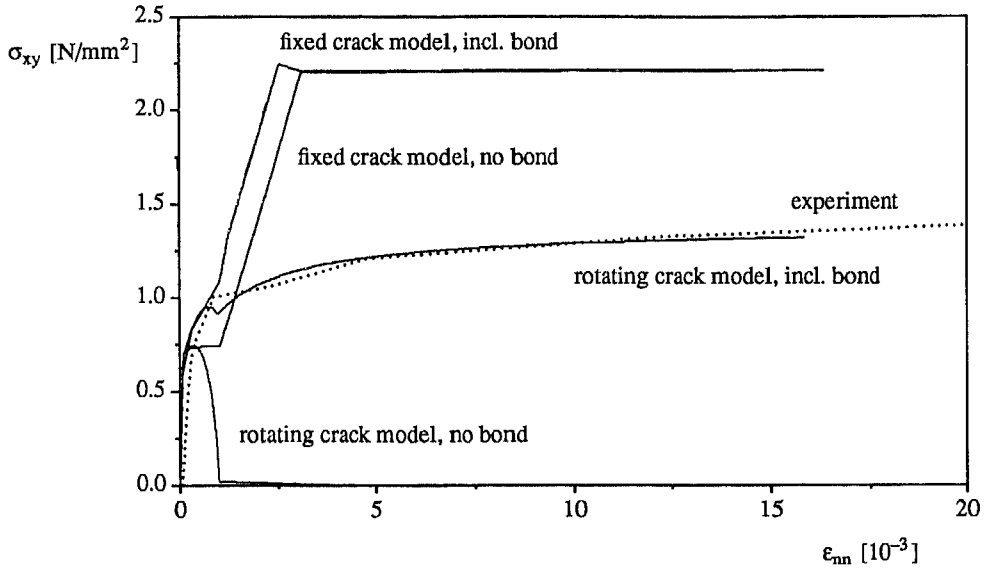

Figure 6 Shear stress - principal tensile strain response for panel PB21.

crack models embedded in a total strain concept are conceptually simple and less CPU consuming than the crack models embedded in a decomposed strain concept.

The results of the simulation of the reinforced panel demonstrate the capability of the presented model for simulating reinforced concrete behavior. Further research is necessary on the constitutive components of the model. The main advantage of the proposed model is the separate treatment of the softening behavior of the concrete and the tension-stiffening behavior of the reinforced concrete due to bond stresses between the cracks.

7. Acknowledgements

The calculations have been carried out with the DIANA finite element code of the Netherlands Institute for Applied Scientific Research, Building and Construction Research (TNO-BOUW). The research was supported financially by the Netherlands Technology Foundation (STW) under grant DCT-77.1405 and by committee A30 "Concrete Mechanics" of the Netherlands Organization for Research, Codes and Specifications (CUR A30).

8. References

Bažant, Z.P. (1983). Comment on orthotropic models for concrete and geomaterials. **J. Engrg. Mech.** , ASCE, 109(3), 849-865.

Bažant, Z.P. and Oh, B.H. (1983). Crack band theory for fracture of concrete. **Materials and Structures**, RILEM, 93(16), 155-177.

Bhide, S.B. and Collins, M.P. (1987). Reinforced concrete elements in shear and tension. Publication 87-02, Univ. of Toronto, Dept. of Civil Engrg., Canada.

de Borst, R. and Nauta, P. (1985). Non-orthogonal cracks in a smeared finite element model.

Eng. Comput. , (2), 35-46.

Cervenka, V.,Pukl, R. and Eligehausen, R. (1990). Computer simulation of anchoring technique in reinforced concrete beams, in **Proc. Int. Conf. Computer Aided Analysis and Design of Concrete Structures** , Part I, eds. N. Bićanić et al., Pineridge Press, Swansea, 1-21.

Crisfield, M.A. and Wills, J. (1989). Analysis of R/C panels using different concrete models. **J. Engrg. Mech.** , ASCE, 115(3), 578-597.

Feenstra, P.H. (1991). Modeling of reinforced concrete panels. Report 25.2.91-5-2, Delft University of Technology, Delft, Netherlands.

Rots, J.G., Nauta, P., Kusters, G.M.A. and Blaauwendraad, J. (1985). Smeared crack approach and fracture localization in concrete. **Heron** , 30(1), 3-48.

Rots, J.G. (1988). **Computational modeling of concrete fracture.** Dissertation, Delft University of Technology, Delft, Netherlands.

Willam, K.J., Pramono, E. and Sture, S. (1987). Fundamental issues of smeared crack models in **Proc. SEM/RILEM Int. Conf. Fracture of Concrete and Rock** , eds. S.P. Shah et al., Houston, 142-157.